

pp. 633-636, 1973.

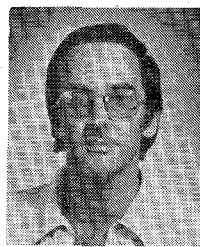
[8] P. H. Masterman and P. J. B. Clarricoats, "Computer field-matching solution of waveguide transverse discontinuities," *Proc. Inst. Elec. Eng.*, vol. 118, pp. 51-63, 1971.

[9] R. Mittra, "Relative convergence of the solution of a doubly infinite set of equations," *J. Res. Natl. Bur. Stand., Sect. D*, vol. 67D, pp. 245-254, 1963.

[10] S. W. Lee, W. R. Jones, and J. J. Campbell, "Convergence of numerical solutions of iris-type discontinuity problems," *IEEE Trans. Microwave Theory Tech.*, vol. MTT-19, pp. 528-536, 1971.

[11] B. MacA. Thomas, "Theoretical performance of prime-focus paraboloids using cylindrical hybrid-mode feeds," *Proc. Inst. Elec. Eng.*, vol. 118, pp. 1539-1549, 1971.

[12] I. S. Gradshteyn and I. W. Ryzhik, *Tables of Integrals, Series and Products*, New York: Academic, 1965, p. 634.



Graeme L. James was born in Dunedin, New Zealand, on September 11, 1945. He received the B.E. and Ph.D. degrees in electrical engineering from the University of Canterbury, Christchurch, New Zealand, in 1970 and 1973, respectively.

Between 1973 and 1976 he was a post-doctoral Fellow with the Department of Electrical and Electronic Engineering, Queen Mary College, London, England, where he was involved in a number of projects concerned with electromagnetic scattering and diffraction and wrote his book *Geometrical Theory of Diffraction for Electromagnetic Waves*. Since June 1976 he has been with the Division of Radiophysics, CSIRO, Sydney, Australia where he has been mainly concerned with research into high performance microwave antennas.

Surface Waves and their Relation to the Eigenfrequencies of a Circular-Cylindrical Cavity

J. V. SUBRAHMANYAM, GREGORY A. H. COWART, MUSTAFA KESKIN, HERBERT ÜBERALL, GUILLERMO C. GAUNAURD, AND EUGENIA TANGLIS

Abstract—The eigenfrequencies of a finite-length cylindrical cavity may be interpreted as the resonances caused by the phase-matching of circumferential waves that circumnavigate the cavity along certain helical paths, and that get reflected back and forth from its top and bottom flat surfaces. In this paper, we obtain the dispersion curves of these circumferential waves that correspond to a series of well-defined pitch angles of their helix for different values of the cylindrical cavity's length-to-radius ratio.

I. INTRODUCTION

THE ANALYSIS of electromagnetic cavity resonators has been the subject of much previous work [1]. We shall consider here the case of a finite cylindrical cavity in

a conducting medium, for which the Dirichlet boundary condition at its surface leads to transverse magnetic (TM) wave propagation, and the Neumann boundary condition leads to transverse electric (TE) wave propagation [2].

The exact expressions [2] for the finite cylindrical cavity's eigenfrequencies corresponding to the two mentioned cases are obtained in the conventional way from satisfying the appropriate boundary conditions. Consider the cavity to be filled with a uniform nondissipative medium having dielectric constant ϵ and permeability μ . With a harmonic time dependence $e^{-i\omega t}$ for the fields inside the cavity, the Maxwell equations yield

$$(\nabla^2 + k^2)\mathbf{E} = 0 \quad (\nabla^2 + k^2)\mathbf{B} = 0 \quad (1a)$$

$$k = \mu\epsilon\omega^2/c_0^2 \quad (1b)$$

where c_0 is the speed of light in *vacuo*. The results come out in terms of standing waves with half-integer multiples of the axial wavelength along the cylinder's length and with integer multiples of azimuthal wavelength around the cylinder's circumference, while the radial boundary condition introduces the roots of the Bessel functions. If the corresponding solutions for the surface field of the cavity are transformed using the Watson-Sommerfeld method, they

Manuscript received January 9, 1981; revised April 30, 1981. The work of J. V. Subrahmanyam and H. Überall was supported by the Naval Air Systems Command under Grant AIR-310B, and the work of G. C. Gaunaurd, E. Tanglis, and H. Überall was supported by the Naval Surface Weapons Center's Independent Research Board.

J. V. Subrahmanyam, G. Cowart, and M. Keskin, are with the Department of Physics, The Catholic University of America, Washington, DC 20064.

H. Überall is with the Department of Physics, The Catholic University of America, Washington, DC 20064, and with the Naval Surface Weapons Center, White Oak, Silver Spring, MD 20910.

G. C. Gaunaurd and E. Tanglis are with the Naval Surface Weapons Center, White Oak, Silver Spring, MD 20910.

can be shown [3], in the high-frequency region, to describe surface waves which propagate around the cylinder along helical Fermat paths. It will be seen in the following that using this surface wave picture, one may obtain dispersion curves for the phase velocities of these surface waves directly from the conventional expressions for the cylinder eigenfrequencies, thereby foregoing the application of the cumbersome Watson-Sommerfeld method. Dispersion curves are found for different length-to-radius ratios and for various pitch angles of the helical paths, which are shown to take on a series of well-defined discrete values.

The motivation for the present study was given by the desire to provide a physical picture, i.e., in terms of surface waves which close into themselves after each circumnavigation, for explaining the cavity resonances and eigenfrequencies conventionally obtained from the normal-mode approach, which is devoid of any comparable physical interpretation. In scattering theory, it is well known [4] that both the modal and the surface wave approach complement each other, the former being more useful at low frequencies where few modes are present, the latter at high frequencies where many modes, but only a few surface waves are important (although each of these two pictures is separately valid, and mathematically equivalent to the other one, over the entire frequency range). In waveguide theory, the surface wave picture seems to have received little attention so far, so that our interpretation of the cavity eigenfrequencies may represent a fairly novel approach in this domain.

II. THEORY

Introducing the interior cavity fields $\psi = E_z$ for TM modes, or $\psi = B_z$ for TE modes (i.e., the field components parallel to the cavity axis z), (1) may be transformed [2] into a transverse wave equation

$$(\nabla_t^2 + \gamma^2)\psi = 0 \quad (2a)$$

where

$$\nabla_t^2 = \nabla^2 - \frac{\partial^2}{\partial z^2} \quad (2b)$$

$$\gamma^2 = \mu\epsilon \frac{\omega^2}{c_0^2} - k_z^2 \equiv k^2 - k_z^2 \quad (2c)$$

with k_z being the longitudinal wavenumber since the fields have a z -dependence $\exp(\pm ik_z z)$, and γ being a transverse wavenumber.

The transverse wave equation (2a), may for the case of a circular-cylindrical cavity, be written as

$$\frac{1}{\rho} \frac{\partial}{\partial \rho} \left(\rho \frac{\partial \psi}{\partial \rho} \right) + \frac{\partial^2 \psi}{\partial \varphi^2} + \gamma^2 \psi = 0. \quad (2d)$$

The solution of this equation leads to separated solutions of (1a) of the form

$$\psi(\rho, \varphi, z) \equiv R(\rho) \Phi(\varphi) Z(z) \quad (3a)$$

where (ρ, φ, z) are the cylindrical coordinates, and the

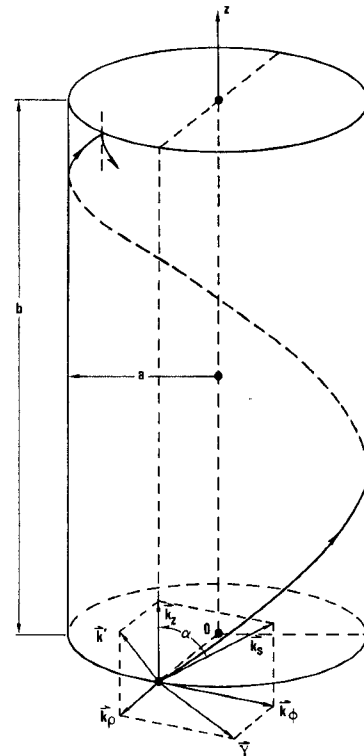


Fig. 1. Finite length cylindrical cavity showing the various components of the propagation vector. (k_s is the propagation vector of the helical Fermat path of the surface wave.)

separated functions are

$$R(\rho) = J_m(\gamma\rho) \quad (3b)$$

$$\Phi(\varphi) = e^{\pm ik_\varphi a\varphi} \quad (3c)$$

$$Z(z) = e^{\pm ik_z z}. \quad (3d)$$

The single-valuedness condition under $\varphi \rightarrow \varphi + 2\pi$ leads to

$$k_\varphi = m/a, \quad m = 1, 2, 3, \dots \quad (4a)$$

which is a condition stipulating that an integer number m of azimuthal wavelengths $\lambda_\varphi = 2\pi/k_\varphi$ exactly fit the cylinder's circumference $2\pi a$. If the cylinder of length b and radius a is placed with its axis along the coordinate z -axis so that its bottom and top surfaces are at $z=0$ and $z=b$, respectively (Fig. 1), then the boundary conditions, e.g., the Dirichlet condition $\psi|_s = 0$, i.e., $Z(0) = Z(b) = 0$, select a Z -solution of the form $\alpha \sin k_z z$, leading to

$$k_z = j\pi/b, \quad j = 1, 2, 3, \dots \quad (4b)$$

which is a condition stipulating that a half-integer number $j/2$ of axial wavelengths $\lambda_z = 2\pi/k_z$ exactly fit the cylinder's length b . For the Neumann boundary condition $\partial\psi/\partial n|_s = 0$, i.e., $Z(0) = Z(b) = 0$, the Z -solution has a form $\alpha \cos k_z z$, which also leads to the same condition of (4b).

If (3b) and (3c) are inserted into (2d) and the Bessel equation is used, one then finds that the wave equation is satisfied with m given by (4a) and γ given by (2c).

The wave vector \mathbf{k} may now be decomposed into components, as shown in Fig. 1, and a variety of relations can be

formed:

$$k^2 = k_p^2 + k_\varphi^2 + k_z^2 \quad (5a)$$

$$k_s^2 = k_\varphi^2 + k_z^2 \quad (5b)$$

$$k^2 = k_p^2 + k_s^2 \quad (5c)$$

$$\gamma^2 = k_p^2 + k_\varphi^2 = k^2 - k_z^2 \quad (5d)$$

the latter condition containing (2c). This analysis shows the interesting fact that the wavenumber γ contained in the radial Bessel function solution is not actually a purely radial wavenumber, but has a tangential component k_φ in it.

The Dirichlet boundary condition (TM mode) $\psi|_s = 0$, at $\rho = a$, leads to the solution

$$\gamma = x_{mn}/a, \quad n = 1, 2, 3, \dots \quad (6a)$$

and the Neumann boundary condition $\partial\psi/\partial n|_s = 0$ at $\rho = a$ to

$$\gamma = x'_{mn}/a, \quad n = 1, 2, 3, \dots \quad (6b)$$

where x_{mn} and x'_{mn} are the n th zeroes of $J_m(x)$ and $J'_m(x)$, respectively. The eigenvalues of the wave vector \mathbf{k} , which are simply related to the eigenfrequencies f of the cavity by $k = 2\pi f/c$ where $c = c_0/\sqrt{\epsilon\mu}$ is the velocity of light in the cavity filler, are now obtained from $k^2 = (\gamma^2 + k_z^2)^{1/2}$. The result for the TM mode (Dirichlet boundary condition) is

$$(ka)_{nmj}^{\text{TM}} = [x_{mn}^2 + (j\pi)^2(a/b)^2]^{1/2} \quad (7a)$$

and for the TE mode (Neumann boundary condition), it is

$$(ka)_{nmj}^{\text{TE}} = [x'_{mn}^2 + (j\pi)^2(a/b)^2]^{1/2}. \quad (7b)$$

Using the abovementioned results of the Watson-Sommerfeld transformation, we now view the surface fields of the cavity as a superposition of helically propagating waves with propagation vector \mathbf{k}_s , and introduce their phase velocities by $c_s = \omega/k_s$. Then the dispersion curves of the surface waves are obtained from

$$c_s/c = (ka)/(k_s a). \quad (8)$$

The right-hand side of (8) is only known at the discrete eigenfrequencies of the cavity but in practice, this information suffices to determine the continuous dispersion curves of the surface waves. At the resonances, the quantity ka is given by (7a) or (7b), and the eigenvalues of $k_s a$ are found from (5b) as

$$(k_s a)_{mj} = [m^2 + (j\pi)^2(a/b)^2]^{1/2}. \quad (9)$$

The points on the dispersion curves which correspond to the cylinder resonances are, therefore, obtained as

$$(c_s/c)_{nmj}^{\text{TM}} = \{[x_{mn}^2 + (j\pi)^2(a/b)^2]/[m^2 + (j\pi)^2(a/b)^2]\}^{1/2} \quad (10a)$$

for the TM modes, and

$$(c_s/c)_{nmj}^{\text{TE}} = \{[x'_{mn}^2 + (j\pi)^2(a/b)^2]/[m^2 + (j\pi)^2(a/b)^2]\}^{1/2} \quad (10b)$$

for the Neumann condition. Equations (10) determine, at a series of discrete points, the phase velocities c_s of the surface waves which propagate along a helical path with pitch angle α (Fig. 1). A collection of paths with discrete pitch angle values α_{mj} is selected by the boundary conditions, where

$$\tan \alpha_{mj} = k_\varphi/k_z = (m/j\pi)(b/a) \quad (11)$$

showing that a surface wave propagating at a given pitch angle corresponds to a constant value of the ratio m/j of eigenfrequency indexes. To each such ratio, there corresponds an infinite series of surface waves which are labeled by the same index n that also labels the order of the zeros of the Bessel function. The discrete pitch angles are determined by the conditions of integer azimuthal wavelength and half-integer axial wavelength, the latter condition corresponding in the surface wave picture, to a back-and-forth reflection of the surface waves from the end caps of the cylinder. We note further that the correction terms due to the pitch of the helix, given by the second terms inside the square brackets of (7), (9), and (10) are not present in the case of normal incidence ($j=0$). For infinite cylinders ($b \rightarrow \infty$) they are still present for the case of helical paths if with the condition $b \rightarrow \infty$, we have simultaneously $j \rightarrow \infty$. Rewriting (11) as

$$m \cot \alpha_{mj} = j\pi(a/b) \quad (12a)$$

then (7), (9) can be arranged as follows:

$$(k_s a)_{mj} = m(1 + \cot^2 \alpha_{mj})^{1/2} \equiv m \csc \alpha_{mj} \quad (12b)$$

$$(ka)_{nmj}^{\text{TM}} = [x_{mn}^2 + m^2 \cot^2 \alpha_{mj}]^{1/2} \quad (12c)$$

$$(ka)_{nmj}^{\text{TE}} = [x'_{mn}^2 + m^2 \cot^2 \alpha_{mj}]^{1/2}. \quad (12d)$$

Hence,

$$(c_s/c)_{nmj}^{\text{TM}} = [(x_{mn}/m)^2 \sin^2 \alpha_{mj} + \cos^2 \alpha_{mj}]^{1/2} \quad (13a)$$

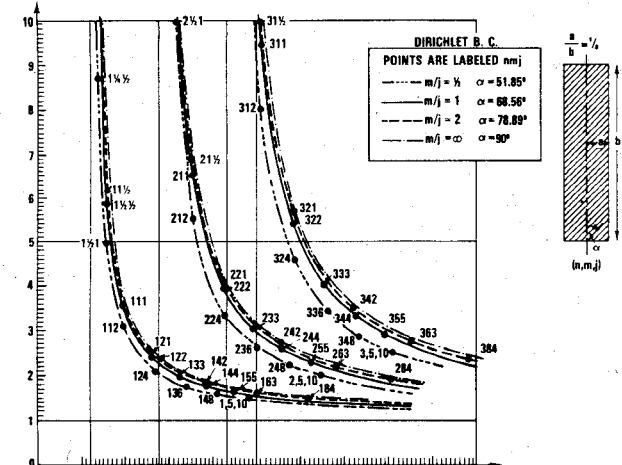
$$(c_s/c)_{nmj}^{\text{TE}} = [(x'_{mn}/m)^2 \sin^2 \alpha_{mj} + \cos^2 \alpha_{mj}]^{1/2}. \quad (13b)$$

For the case of Neumann boundary conditions, the usual interpretation of the surface waves in terms of "Whispering Gallery" waves [4] which reflect successively from the inner cylinder surface can be carried through in a straightforward manner.

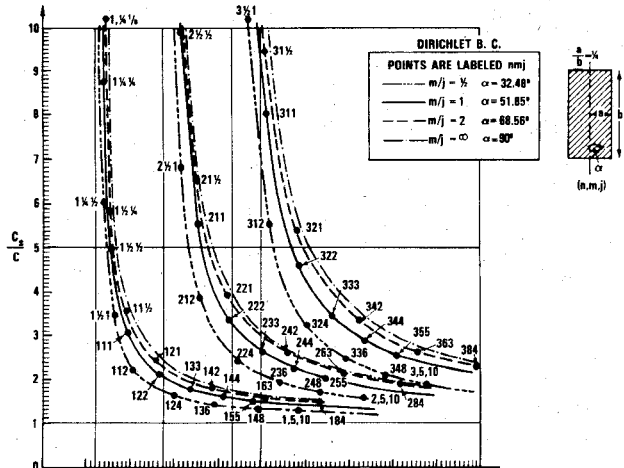
III. DISPERSION CURVES OF THE SURFACE WAVES

We have carried out numerical calculations of the dispersion curves for the helical surface waves on cylindrical cavities with various values of the radius-to-length ratio

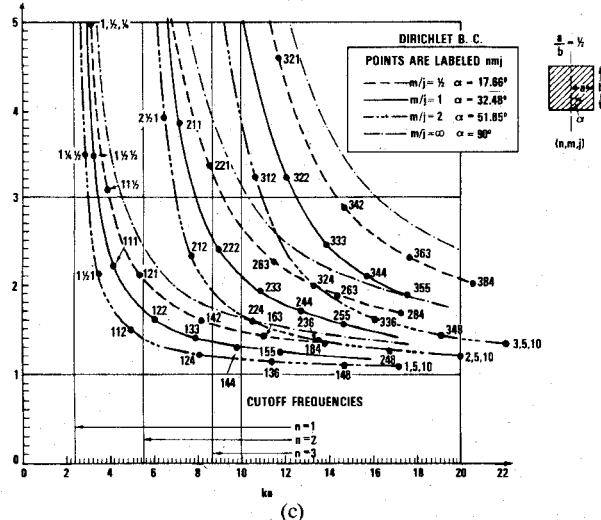
a/b , obtaining the discrete points from (10). These points were spaced sufficiently closely so that smooth curves could be drawn through them. Fig. 2 shows the dispersion curves (i.e., the c_s/c values) plotted versus wave size ka for a cylindrical cavity satisfying the Dirichlet boundary con-



(a)



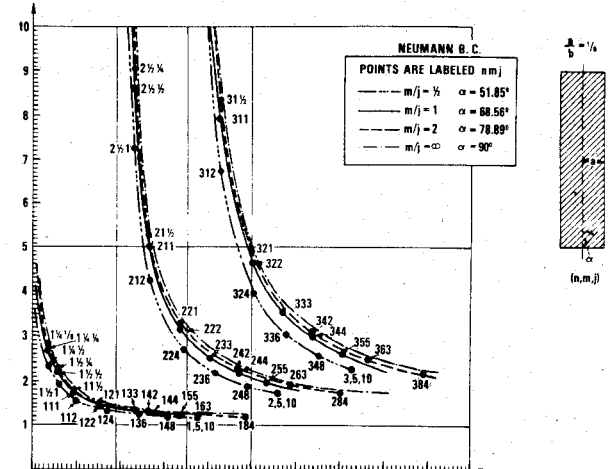
(b)



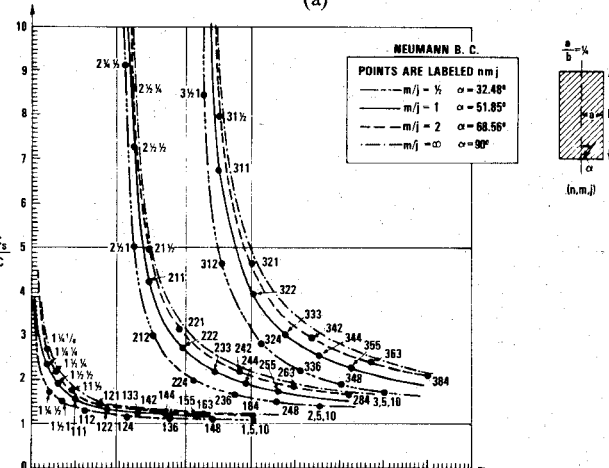
(c)

Fig. 2. (a) Dispersion curves of heliocoidally propagating surface waves on a long finite cylindrical cavity ($b/a=8$), corresponding to four different pitch angles determined by the ratios $m/j = 1/2$, (dash-dotted curve), 1 (solid curve), 2 (dashed curve) and ∞ ($\alpha = 90^\circ$, dotted curve) as indicated, for TM modes satisfying the Dirichlet boundary condition on the surface. (b) Same as Fig. 2(a) for a shorter ($b/a=4$) cavity. (c) Same as Fig. 2(a) for an even shorter ($b/a=2$) cavity.

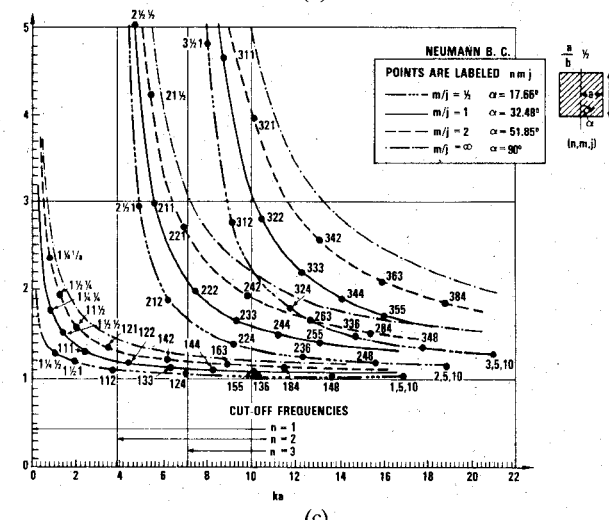
dition (i.e., TM modes). Fig. 3 shows analogous curves for the cylindrical cavity satisfying the Neumann condition (i.e., TE modes). Each figure consists of three parts corre-



(a)



(b)



(c)

Fig. 3. (a) Same as Fig. 2(a), but for TE modes satisfying a Neumann boundary condition on the cavity surface. (b) Same as Fig. 2(b), but with a Neumann boundary condition. (c) Same as Fig. 2(c), but with a Neumann boundary condition.

sponding to a/b ratio of (a) $1/8$, (b) $1/4$, and (c) $1/2$, and the corresponding cylinder shapes are sketched in the figures. The discrete points along the curves correspond to the discrete cavity eigenfrequencies and are labeled by the set of three integers n, m, j . The integer n labels the entire

curve which, therefore, refers to the n th member of the surface wave family that propagates around the cylindrical cavity along a helical Fermat path with a given pitch angle α_{mj} .

It follows from (11) that this angle is determined by the ratio of the integer labels m and j , which stays constant along each dispersion curve. Each of these figures exhibits four curves corresponding to m/j ratios of $1/2$ (dash-dotted), 1 (solid), 2 (dashed), and ∞ ($\alpha=90^\circ$, dotted) with the corresponding pitch angles α_{mj} quoted on the graphs. These α -angles vary depending on the values of the a/b ratio (except for $\alpha=90^\circ$ where c_s/c is independent of a/b), and inspection of Fig. 1 shows that the more elongated the cavity becomes, the tighter the helix is wound for a given value of the m/j ratio. In other words, the shorter the cavity the more often a surface wave of fixed m/j value will be reflected back and forth between the two flat end surfaces. Dispersion curves have been produced only for the indicated values of α , but the dependence on the value of α is seen to be weak; there is a much stronger dependence on the a/b value. The leftmost points on the curves are (n, m, j) with one of m or j equal to unity. The smooth curves drawn through these points, which rise to an infinite cutoff at appropriate cutoff frequencies, may however be obtained by an extrapolation of (10) with m treated as a continuous variable. The cutoff frequencies are obtained for $m \rightarrow 0$, since (13) show that then, $(c_s/c) \rightarrow \infty$ (note that j/m and hence α_{mj} is constant along each dispersion curve); thus

$$\begin{aligned} (ka)_{nmj}^{\text{TM}} &= x_{0n} \\ (ka)_{nmj}^{\text{TE}} &= x'_{0n} \end{aligned} \quad (14)$$

determine the cutoff frequency. This limit is the same for all values of j/m , i.e., for any pitch angle.

Fig. 1 may provide the impression that our formalism is based on a ray picture of the diffraction process, which would be valid only for large values of ka . The dispersion curves which our formalism provides are, however, obtained from the wave equation and thus, are valid for all frequency ranges down to the cutoff frequencies.

The high-frequency limit of our dispersion curves is obtained by noting that along each curve, $m \rightarrow \infty$, $j \rightarrow \infty$, (with $m/j = \text{constant}$) in that limit. Using (13) and noting that [5]

$$\lim_{m \rightarrow \infty} x_{mn} \rightarrow m \quad \lim_{m \rightarrow \infty} x'_{mn} \rightarrow m \quad (15a)$$

it becomes apparent that

$$\lim_{ka \rightarrow \infty} (c_s/c)_{nmj} = 1. \quad (15b)$$

Figs. 2 and 3 bear out this conclusion.

We should also comment on the case of the pitch angle $\alpha_{mj} = 90^\circ$, so that the corresponding surface wave describes a circular, rather than helical, path over the cylinder surface. This case corresponds to $j=0$, i.e., $k_z=0$, and thus $m/j=\infty$. Equations (10) show that then

$$\left(\frac{c_s}{c} \right)_{nm0}^{\text{TM}} = \frac{x_{mn}}{m} \quad (16a)$$

and

$$\left(\frac{c_s}{c} \right)_{nm0}^{\text{TE}} = \frac{x'_{mn}}{m} \quad (16b)$$

while the corresponding ka -values are

$$(ka)_{nm0}^{\text{TM}} = x_{mn} \quad (17a)$$

$$(ka)_{nm0}^{\text{TE}} = x'_{mn}. \quad (17b)$$

These results are seen to be independent of the cavity's a/b ratio, and they are plotted as the dotted curves in Figs. 2 and 3.

The case of an infinitely long cylindrical cavity, $b \rightarrow \infty$, should also be considered. Since k_z of (4b) has to remain finite for this case, we must then also require that $j \rightarrow \infty$, so that k_z becomes a continuous variable. Accordingly, from (11), the pitch angle $\alpha_{m\infty}$ is then no longer quantized and becomes a continuous quantity also, given by

$$\tan \alpha_{m\infty} = m/(k_z a) \quad (18)$$

but it corresponds to different sets of continua corresponding to the values of m . To obtain dispersion curves, (12) and (13) can be used with α_{mj} replaced by the continuous angle $\alpha_{m\infty}$. Figs. 2 and 3 still represent examples even for the case of the infinite cylinder, but with particular choices of the pitch angle.

Finally, we note that some typical features of solutions of Neumann and Dirichlet problems become quite apparent from the graphs. All curves of a given case for the Neumann boundary condition always lie beneath the corresponding ones for the Dirichlet boundary condition, thus, in the Neumann case all surface waves have correspondingly slower phase velocities than in the Dirichlet case. Moreover, for all cases shown in Figs. 2 and 3, the dispersion curves for the Neumann case (Fig. 3) are interlaced, for all cavity lengths (i.e., solid, dashed, and dotted curves), with the respective ones of the Dirichlet case (shown in Fig. 2). This means, for example, that the solid (dashed or dotted) curves having first index $n=2$ in Fig. 2(a), 2(b), or 2(c) lie between the solid (dashed or dotted) curves having first indexes $n=2$ and $n=3$ in Fig. 3(a), 3(b), or 3(c), respectively. Eigenvalue interlacing theorems to this effect could be shown to hold.

IV. SUMMARY AND DISCUSSION

We have employed the picture of helically propagating surface waves on a cylindrical cavity of finite length, obtained via the Watson-Sommerfeld method [3], in order to generate, in a very simple fashion, the dispersion curves of the surface waves. These creeping waves propagate along helicoidal Fermat paths with fixed pitch angle α . Their phase velocities were computed at a series of discrete points which were close enough to permit the drawing of continuous interpolating dispersion curves through them. These points correspond to the locations of the cavity eigenfrequencies and we have restricted our analysis to the case of a cavity with perfectly conducting walls. In this case, explicit expressions for the eigenfrequencies are known and can be determined by a Dirichlet (TM modes) or by a Neumann (TE modes) boundary conditions on its surface.

The surface wave picture brings a new order into the variety of eigenfrequencies of a cavity. Instead of m , the mode number and order of the Bessel function solution of the guide, it is now the integer n which is the predominant index since it labels the individual surface waves. The other two labels m and j are seen to have geometrical significance only since they tell us, essentially through (5b) in conjunction with (4a) and (4b) (which may also be rewritten in terms of the wavelengths along the φ - and z -direction, i.e.,

$$(1/\lambda_s)^2 = (1/\lambda_\varphi)^2 + (1/\lambda_z)^2 \quad (19)$$

where λ_s is the wavelength of the surface wave), exactly in which geometrical fashion the n th surface wave is located on the cavity surface. Equation (19) is an expression of the fact that, with $m\lambda_\varphi = 2\pi a$ and $j\lambda_z = 2b$, the surface waves are actually closed into themselves (and thus cause the modal fields in a resonant fashion) after completing their helical path, including the back-and-forth reflections from the ends of the cylinder.

In this connection, it is worth noting that the "surface waves" of our terminology extend in fact into the interior of the cavity (although they are more easily visualized on the surface). But as mentioned before, this picture is most useful at high frequencies where large mode orders m are encountered; and in this regime, the Bessel function field solutions of (3b) are most heavily weighted towards the surface of the cavity [4]. We also note that the surface wave picture with its accompanying reclassification and physical interpretation of the cavity resonances does arise mathematically from a full-fledged use of the Watson transformation [3], but that our present approach, based only on the actual resonance frequencies, has achieved the same results in a vastly simpler fashion.

Some further discussion of the relation between normal modes and our surface waves (here loosely pictured as rays, for illustrative purposes) might be in order. There is no strict one-to-one correspondence of one mode to one ray *per se*. There is, however, a connection between a ray and some "representative" modes. This connection may be gleaned from a paper by Tindle and Guthrie and their discussion of sound propagation in an inhomogeneous oceanic wave guide [6]. A ray picture emerges at high frequencies where many modes m, j are available to form a superposition. The weight factors of this superposition are known if the manner of exciting the fields in the guide is prescribed (in [6], this was provided by a point source). If a partial sum centered around the mode with labels m_0, j_0 is selected out of the modal sum, Tindle and Guthrie showed using WKB theory and also by numerical calculation that the field defined by such a partial sum approximately represented a ray corresponding (for the present case) to a geometry given by (11), i.e., to

$$\tan \alpha_{m_0 j_0} \equiv (m_0 / j_0 \pi) (b/a). \quad (20a)$$

At high frequencies, many modes are available to form the partial sum and the field resembles a fairly sharp, well-defined ray. At low frequencies, the few modes available can only form a fuzzy kind of ray. This was also demonstrated in the acoustic model experiments of A. B. Wood

where these fuzzy rays were optically visualized [7].

At a given point on the surface of the cavity (or, to that effect, anywhere in its interior), the field of a representative mode (m_0, j_0) , in the aforementioned sense, actually corresponds to four different helical waves: a counter-rotating pair with pitch angles $\pm \alpha_{m_0 j_0}$ for a cylindrical waveguide, and for the cavity, two such pairs propagating in the $+z$ - and $-z$ -directions, respectively. Note, however, that this picture of "rotating" waves has nothing to do with any "circular polarization" of the helical wave fields; the ray picture rather refers to the (helical) direction of energy flow contained in the modal group centered around (m_0, j_0) which corresponds to the given helical field, while the polarization of this group of modes follows from standard wave guide theory [1].

It is believed that our present discussion of helical waves introduces a novel point of view into the subject of wave guides and resonant cavities, which due to the physical picture it furnishes, and due to the simple connection between cavity eigenfrequencies and helical-wave resonances upon which we have elaborated here, has presented us with some worthwhile new insights.

REFERENCES

- [1] See, e.g., G. Goubau, *Electromagnetic Waveguides and Cavities*. New York: Pergamon, 1961.
- [2] See, e.g., J. D. Jackson, *Classical Electrodynamics*. New York: Wiley, 1962.
- [3] See, e.g., for the scalar case, M. C. Junger, *J. Acoust. Soc. Amer.* vol. 41, p. 1336, 1967.
- [4] See, e.g., H. Überall, "Surface waves in acoustics," in *Physical Acoustics*, W. P. Mason and R. N. Thurston, Eds., New York: Academic, 1973, vol. X, p. 40.
- [5] *Handbook of Mathematical Functions*, ed. M. Abramowitz and I. Stegun (Government Printing Office, Nat. Bureau of Standards, Washington, DC, 1964), Ed. 9.5.16, 16.
- [6] C. T. Tindle and K. M. Guthrie, *J. Sound Vib.*, vol. 34, p. 291, 1974.
- [7] See I. Tolstoy and C. S. Clay, *Ocean Acoustics*. New York: McGraw-Hill, 1966.

+

J. V. Subrahmanyam was born in Vizianagaram, India, on August 4, 1943. He received the B.E. and M.E. degrees in mechanical engineering from Andhra University, Waltair, India, in 1964 and 1966, respectively. In March 1980 he joined The Catholic University of America, Washington, DC, as a graduate assistant in physics.

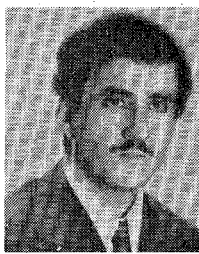
He was Lecturer in mechanical engineering at the Osmania University from 1966 to 1980.

+

Gregory A. H. Cowart was born in Buenos Aires, Argentina, on January 3, 1950. He received the B.A. degree in mathematics in 1978 from the University of West Florida, Pensacola, FL. Presently, he is a doctoral candidate at The Catholic University of America, Washington, DC.

His interests include electromagnetic scattering from inhomogeneous objects with irregular boundaries.





Mustafa Keskin was born December 2, 1955, in Artvin, Turkey. He received the B.E degree in engineering physics in 1976 from the Black Sea Technical University, Trabzon, Turkey. Since 1977 he is on a scholarship awarded by the Government of Turkey studying for the M.S. and Ph.D. degrees at the Catholic University of America. He received the M.S. degree in physics in 1980 from the Catholic University of America. He is currently working on the Ph.D. degree at the same institution.

His main interests are in electromagnetic theory.

+

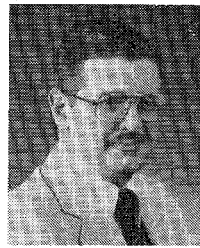


Herbert Überall (M'80) was born October 14, 1931 in Neunkirchen, Austria. He received the Ph.D. degree from the University of Vienna, Vienna, Austria, in 1953, and the Ph.D. degree from Cornell University, Ithaca, NY, in 1956, both in theoretical physics.

He has been Assistant Professor of Physics at the University of Michigan from 1960 to 1964, Associate Professor at the Catholic University of America, Washington, DC, and Professor of Physics at that institution since 1965. He has been Consultant to the Conduction Corporation, Ann Arbor, MI, during 1961-1964, Consultant to the Naval Research Laboratory since 1966, and Staff Member of the Naval Surface Weapons Center since 1976.

His interests include theoretical nuclear physics in which he authored or coauthored several books, as well as theoretical acoustics and electromagnetic theory. In these latter fields, he has been instrumental, together with several collaborators, in developing the theory of resonance scattering of acoustic, elastic, and electromagnetic waves, and in establishing the connection between these resonance phenomena and the surface waves generated in the scattering process, utilizing the theory of nuclear resonance scattering for such purposes.

Dr. Überall is a Fellow of the American Physical Society and of the Acoustical Society of America, and a member of the International Union of Radio Science (URSI) and the American Association of University Professors (AAUP).



Guillermo C. Gaunaud was born in Havana, Cuba, on July 19, 1940. He received the A.B. degree in mathematics in 1964, the B.S.M.E. degree in 1965, the M.S. degree in applied mechanics in 1967, and the Ph.D. degree in acoustics in 1971, all from Catholic University, Washington, DC.

He was a National Defense Education Act Fellow and an ONR grantee for a five year period as a graduate student. From 1968-1970 he concurrently worked as a Senior Engineer with Litton Industries in College Park, MD. Since 1971 he has been a Research Physicist at the Research Department of the Naval Surface Weapons Center, White Oak, MD, specializing in acoustics. His interests currently include all aspects of wave propagation, radiation, and scattering, particularly the interaction of acoustic and elastic waves with materials and structures. He has authored many papers in these areas including a recent group on the resonance theory of scattering. Since 1978 he has occasionally lectured on acoustics at Catholic University.

Dr. Gaunaud is a Fellow of the Acoustical Society of America, of the Washington Academy of Sciences, and of the American Association for the Advancement of Sciences. He is a member of many professional and honor societies including the New York Academy of Sciences, the American Physical Society, the Philosophical Society of Washington, Sigma Xi, and Tau Beta Pi. His professional biographical sketch has appeared in American Men of Science, Who's Who, and three other analogous books.

+



Eugenia Tanglis was born May 21, 1950 in Cleveland, OH. She received the B.S. degree in physics and mathematics in 1972 from Purdue University, West Lafayette, IN, and the M.S. degree in physics in 1976 from the Catholic University of America, Washington, DC.

She was a Research Physicist at the Naval Surface Weapons Center, White Oak, Silver Spring, MD, since 1972, where she has worked mainly in the field of underwater acoustics, and has published several papers.

Ms. Tanglis is a member of the Acoustical Society of America, Sigma Xi, and Sigma Pi Sigma.